Available online at www.sciencedirect.com

ScienceDirect

Procedia Structural Integrity 37 (2022) 517–524

Structural Integrity Procedia

www.elsevier.com/locate/procedia

ICSI 2021 The 4th International Conference on Structural Integrity

On the exploitation of multiple 3D full-field pulsed ESPI measurements in damage location assessment

Alessandro Zanarini*

DIN, Industrial Engineering Dept., University of Bologna, Viale Risorgimento 2, 40136 Bologna, Italy

Abstract

The structural dynamics of a manufactured part or system is often used as a key player in the discrimination of a sound behaviour or of a defected component, which must not go into service. Many NDT approaches exploit different loading systems to enhance the recognition of defects in components. Among the NDT techniques, Shearography, with its opto-mechanical shearing of electronic speckle pattern interferometry fields, mainly uses the vacuum technology to give a distributed, but static, loading on the sensed surface. Instead, it was already demonstrated that broad frequency excitation can enhance the defects' recognition, as the higher structural dynamics may reveal local anisotropies that are not excited by static loading only, but need tonal signature in the testing deformation source.

In this work the attention is drawn onto the concurrent exploitation of multiple 3D full-field data, obtained by pulsed ESPI displacement measurements with sound pressures and shaker mono-tonal excitations at different frequencies. The usage of multiple data allows to gather the information about different defects that are oddly revealed at single frequency lines. The 3D nature of the datasets plays a relevant role, as the inhomogeneities are more easily detected from the in-plane displacements. Before summing all the available information, the single datasets can be enhanced by thresholding and functionally grading the 3D displacements. The application of the proposed method on a FGRP honeycomb panel, defected on purpose by proper manufacturing, was able to reveal all the know discontinuities by clustered areas of high displacement amplitude, by means of the processed 3D full-field dynamic maps.

Keywords: multiple data processing; 3D full-field dynamic data; damage location

1. Introduction

The breaking idea here proposed was to smartly exploit a broad database of *full-field optical 3D displacement measurements* into a simple damage location routine, working on summing the threshold-emphasised multiple data. Three main assets were of relevance: first, the 3D nature of the fields provided the *in-plane* or *surface-tangent motions*, which already proved in Zanarini (2005b) to be discriminatory in revealing sub-surface anisotropies; second, *different*

* Corresponding author. Tel +39 051 209 3442.
E-mail address: a.zanarini@unibo.it (Alessandro Zanarini).

10.1016/j.prostr.2022.01.117

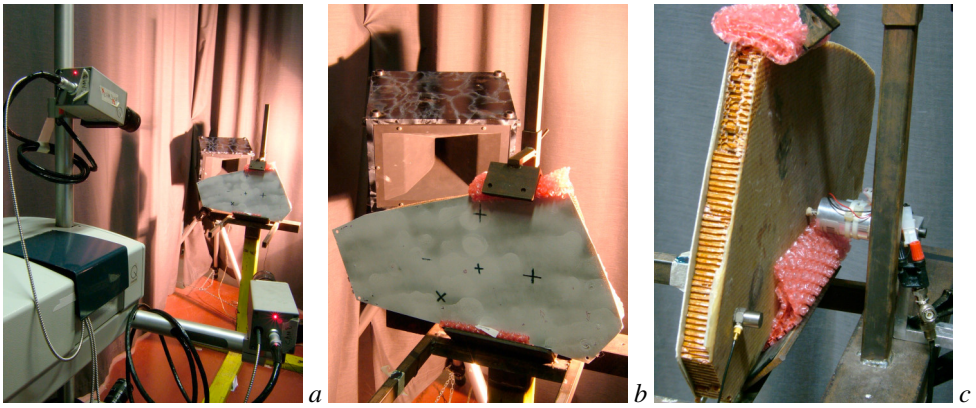

Fig. 1. The *in-situ* testing of the *pre-damaged* FGRP honeycomb panel from Zanarini (2005b), with the pulsed ESPI system in evidence in *a*, the sound wave emitter in *b* and the back positioned shaker in *c*.

excitation sources were used (single tone sound pressure wave, shaker and pre-load), with quite broad frequency content, to be able to excite the local anomalous behaviour of the surface over each specific defect, as none of the excitations, nor frequencies, was able to clearly provide the information for all the defects in a single measurement; third, the *multiplicity of the data* was of great help, as each data provided only partial information, as in the previous point, therefore only a guided gathering resulted in a broad view of the defects' location.

These works are a spin-off of the activities held during the HPMI-CT-1999-00029 *Speckle Interferometry for Industrial Needs* Post-doctoral Marie Curie Industry Host Fellowship project at Dantec Ettemeyer GmbH in years 2004-05. They take also advantage of the the grown experiences that brought to the *Towards Experimental Full Field Modal Analysis* (TEFFMA) project, through the Marie Curie FP7-PEOPLE-IEF-2011 PIEF-GA-2011-298543 grant.

Since the testing in the *Speckle Interferometry for Industrial Needs* project (see Zanarini (2005a,b)) it became self-evident how ESPI measurements could give relevant mapping about the local behaviour for enhanced structural dynamics assessments (see Zanarini (2007)) and fatigue spectral methods (see Zanarini (2008a,b)). The results in the former were the basis for the TEFFMA birth, whose works saw earlier presentations in Zanarini (2014a,b), followed by Zanarini (2015a,b,c,d). In Zanarini (2018) a gathering of the works of TEFFMA was firstly attempted, while in Zanarini (2019a) an extensive description of the whole receptance testing was faced and in Zanarini (2019b) the EFFMA was detailed together with model updating attempts. The works in Zanarini (2020) underlined the higher quality of ESPI datasets in full-field dynamic testing. In Zanarini (2021c) a precise comparison was made about new achievements for rotational and strain FRF maps, where again ESPI proved *higher consistency*, therefore its adoption as the best technique when dealing with *strain processing* to *stress mapping* and *fatigue spectral methods*.

A brief description of the testing is outlined in Section 2, with attention on the set-up, the background of ESPI in NDT and the defected FGRP sample geometry. Section 3 deals with the enhancement of 3D datasets by *normalised thresholding*, with related real test comparisons. Section 4 pertains the interpretation of the results, before Section 5 for the final conclusions.

2. The testing

2.1. Basics of pulsed ESPI in NDT

Some of the benefits of pulsed ESPI as NDT technique can be here recalled from Van der Auweraer et al. (2001) and real testing experience (see Zanarini (2005a,b)): *non contact*, *in-situ* measurements; no need of an undamaged reference nor models; no influence of the environment; no complex surface preparation; no scanning but large areas; nearly any material; high spatial resolution; fast measurements & post-processing; excitation independent.

More insight might be useful about the *speckle pattern origin*: the surface roughness, close to the wavelength of the monochromatic & coherent laser light used, randomly scatters the incident light with an interference effect, generating the so called *speckle pattern*, thus randomly populated by light interference, function of the specific surface state.

Therefore the *speckle pattern* is the carrier of the ESPI measurement. In the Michelson interferometer scheme found in Zanarini (2005a,b), a laser light goes in a *beam splitter* to obtain a *reference* and an *object beam*. The *reference beam* is expanded by a lens, and reflected by another beam splitter to the CCD plane. The *object beam* goes through a lens to illuminate the object with an angle to the *observation direction*. The light scattered back by the surface is collected by a lens and recorded on the CCD. The *superposition* between the *reference* and *object speckles* generates a *pattern of light intensity*, which can be recorded in *states*, with different path length/phase for the *object beam*. If we subtract the *light intensity pattern* of the *deformed state* from the *reference state* one, we obtain the *fringes*, to be further processed by *phase map* extraction techniques (Maas (1991)). The phase difference between the *fringes* is related to the constant *laser wavelength* and the projection of 3D displacement on the *measuring direction*. It follows that ESPI delivers fields of precisely measured displacements on the visible surface. Therefore, any unexpected local inhomogeneity detection in phase or displacement maps becomes the driver of damage location assessment underneath the surface.

2.2. Brief summary of the test set-up

The same *raw* tests were already proposed in the paper Zanarini (2005b). The set-up in Fig.1 was made of a pulsed 3D ESPI unit (Ettemeyer Q600), of a clamped honeycomb defected panel for *in-situ* NDT, and thermal gradients, sound wave emitter, shaker, static pre-load were used as local deformation sources.

The use of 3D measurements, with 3 cameras, or more to enhance the estimation of the sensitivity matrix, augments the sensitivity to local patterns, as later shown in the *in-plane* displacements. Some relevant data of the Ettemeyer Q600 are here recalled: pulsed Ruby laser (694 *nm wavelength*), 1 *m coherence length*; release time less than 10 *ns* per pulse and 2-800μs of pulse adjustable delay to freeze any motion *in-situ*; sensed area up to some m^2, thanks to dedicated lenses; 3 cameras with over 1 MPixels CCD sensors; displacement range of 60 *nm* to 10 μm.

2.3. Pre-defected sample geometry: construction scheme of the FGRP panel

In order to assess the capabilities of the approach, a *pre-defected* 530 x 315 x 40 *mm* FGRP sandwich panel was prepared as in Fig. 2, restrained by 2 clamps, with its precise construction scheme. The front skin of the honeycomb panel is made by 4 layers of epoxy/fiberglass unidirectional cross-ply (the 2nd is inter-winded); a cellulose fiber honeycomb dipped in a resin detaches the back skin, also made of epoxy/fiberglass unidirectional cross-ply.

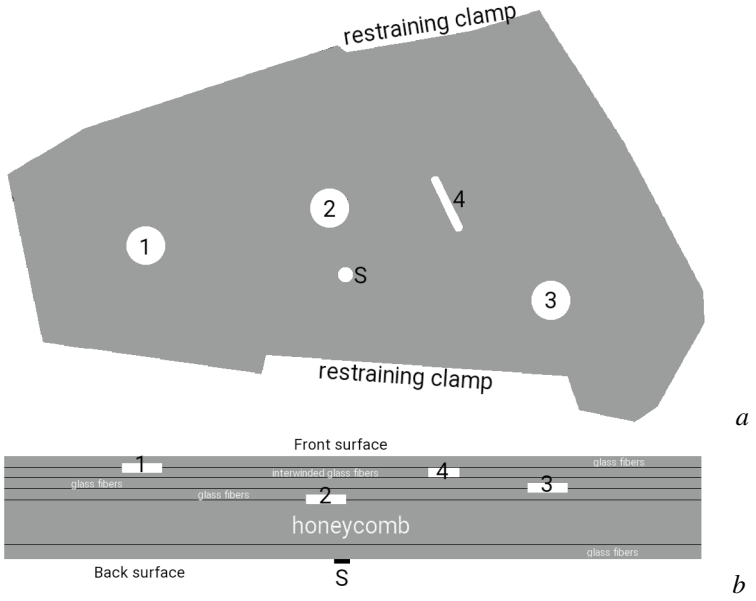

Fig. 2. The *pre-damaged* FGRP honeycomb panel scheme, with the plant of defects' locations in *a* and internal layers' structure in *b*.

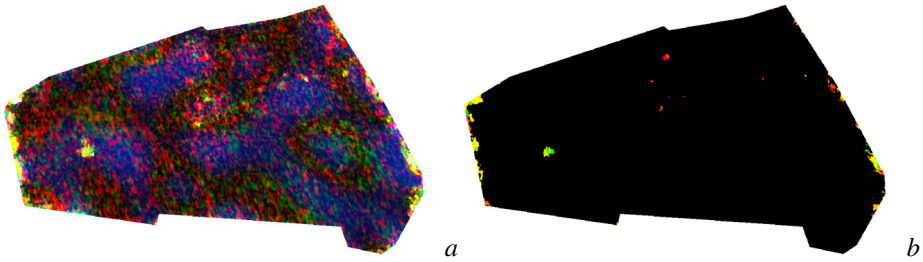

Fig. 3. Comparison of 3D data @ 3675 Hz - *sound pressure wave*: *raw* 3D data in *a*, *normalised thresholded* 3D data in *b*

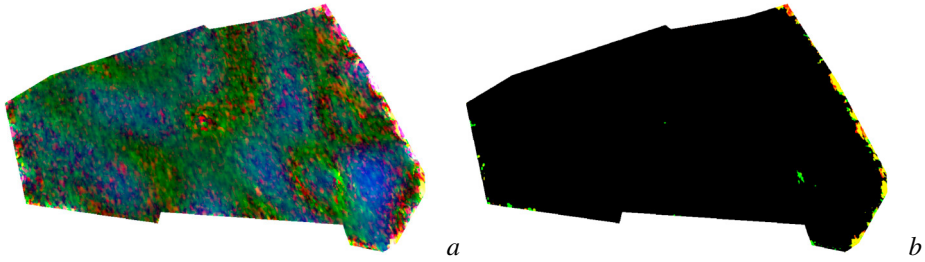

Fig. 4. Comparison of 3D data @ 3925 Hz - *sound pressure wave*: *raw* 3D data in *a*, *normalised thresholded* 3D data in *b*

To simulate typical defects, 3 wax disks of diameter 30mm were inserted among the front skin layers, as in the lower scheme of Fig. 2, before the curing of the sandwich, during which they melted and left voids/discontinuities instead. Defect 1 is superficial, defect 2 is deep close to the honeycomb, defect 3 is intermediate; a wide notch/cut represents defect 4 on the inter-winded glass fibers. Also the location of the shaker is depicted, for further discussion.

3. Enhancement of 3D datasets by *normalised thresholding*

A very simple 3D data enhancement was proposed to raise the info in the defected areas, with great attention to the *in-plane* [X-Y] motions and to the large *multiplicity* of available datasets. This simple approach does not involve any field derivatives as in Araújo dos Santos et al. (2006) or *Shearography*'s equipment as in Lopes et al. (2019). In listing 1 you see the simplification of the C-language code, where the `data*` *below* each `threshold*` are *reduced*, whereas *above* are *emphasised*, all *normalised* with the amplitude (`Amp*`) of each field. Finally, the `Sum*` collect *all* the contributions of this *normalised thresholding* approach.

```
float  thresholdX=0.15,thresholdY=0.15,thresholdZ=0.75, power=2.0; Ndata=11;

for (i=1;i<=Ndata;i++) {
  if ((fabs(dataX) <= thresholdX*AmpX) && (fabs(dataY) <= thresholdY*AmpY) && (fabs(dataZ) <= thresholdZ*AmpZ)){
      dataX*=pow(thresholdX,power)/AmpX;
      dataY*=pow(thresholdY,power)/AmpY;
      dataZ*=pow(thresholdZ,power*power)/AmpZ;
    } else {
      dataX/=pow(thresholdX,power*power)*AmpX;
      dataY/=pow(thresholdY,power*power)*AmpY;
      dataZ/=pow(thresholdZ,power)*AmpZ;
    }
    SumX+=fabs(dataX)*AmpX;
    SumY+=fabs(dataY)*AmpY;
    SumZ+=fabs(dataZ)*AmpZ;
}
```

Listing 1. Example of *normalised thresholding* C-language code

3.1. Real test results' comparisons

The proposed *normalised thresholding* enhancement was applied to *all* the available 3D datasets: in the following 8 pictures it is possible to see on the left the *raw* 3D data and on the right the *processed* ones, when relevant, otherwise

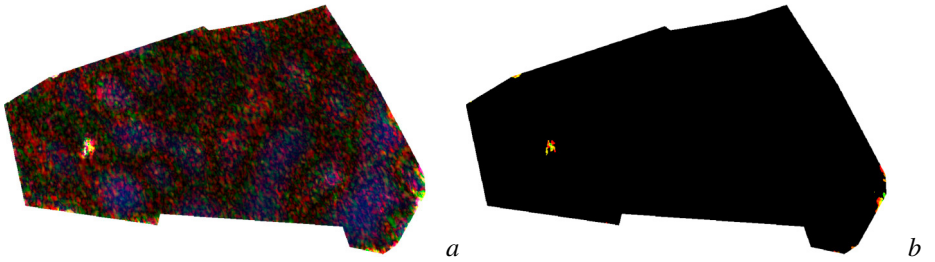

Fig. 5. Comparison of 3D data @ 4575 Hz - *sound pressure wave*: *raw* 3D data in *a*, *normalised thresholded* 3D data in *b*

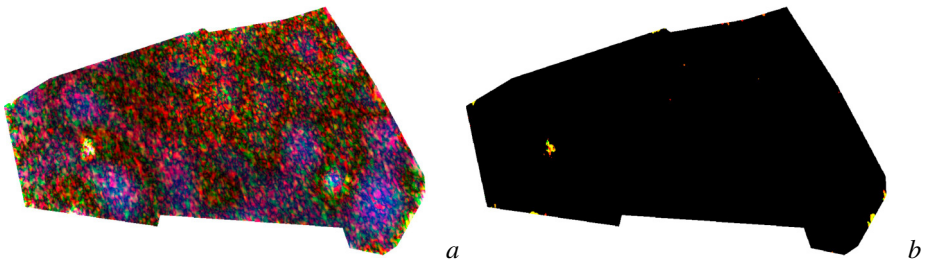

Fig. 6. Comparison of 3D data @ 4750 Hz - *sound pressure wave*: *raw* 3D data in *a*, *normalised thresholded* 3D data in *b*

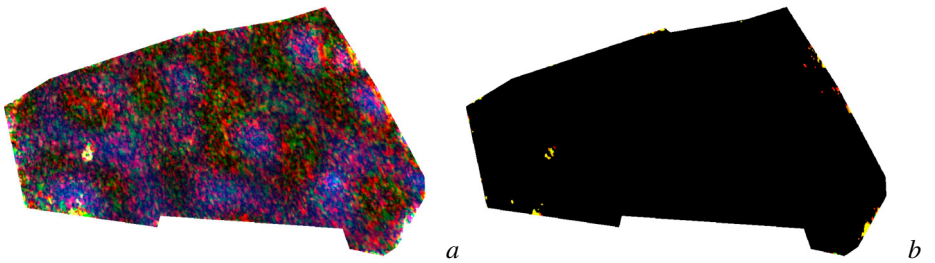

Fig. 7. Comparison of 3D data @ 4800 Hz - *sound pressure wave*: *raw* 3D data in *a*, *normalised thresholded* 3D data in *b*

omitted. Common to all is the pulsed ESPI source and 3D nature of data, where the displacements receive a different colour per direction: [X(red) - Y(green) - Z(blue)], graded by maximal amplitude; what changes is the excitation type and frequency. It is possible to read in Fig.3 at 3675 Hz some information about defect 1, 2; in Fig.4 at 3925 Hz some information about defect 2, 3; in Fig.5 at 4575 Hz some information about defect 1; in Fig.6 at 4750 Hz some information about defect 1, hardly on 3; in Fig.7 at 4800 Hz some information about defect 1; the 3 results at 3375, 5600 and 6200 Hz were here not shown, due to their limited relevance, but cumulated in the `Sum*`. In Fig.8 a shaker is used at 4800 Hz, with strong localisation of the shaker itself, of defect 3, 4, 2, 1 in fading relevance; in Fig.9, again, a shaker at 5600 Hz, with clear localisation of the defect 2, 1, and 3 in much fading relevance; in Fig.10, instead, from the shaker at 5600 Hz plus a static pre-load, some info is caught only in defect 1, but hard to manage on 2 and 3.

Finally, in Fig.11 the *sum* of *all* the *raw* data can be seen, against the `Sum*` of *normalised thresholded* data, from *multiple excitation types* (sound waves, shaker sine, static pre-load) and from *multiple excitation frequencies*. It can be easily appreciated how the *thresholding procedure* augments the clarity towards the useful information for the defects' identification.

4. Interpretation of the results

A close inspection of the results underlines: first, how small defects require *specific* excitations and frequencies to be revealed; second, that the *in-plane* [X - Y] displacements are more sensible to specific local patterns, thus fundamental in witnessing the real structure behaviour under the surface skin; third, that the *multiplicity* of datatsets

extends the chance to sense more anomalies, then potential defects, in the local 3D displacement patterns. In this perspective, it's important to recall that: *multiple* excitation types and frequencies were needed; 11 3D data fields took part to the identification; *in-plane* [X - Y] motion carried the most relevant info for the detection; though, the noise on the borders was related to measurement quality, and might be avoided with stabler technologies.

The main anomalies were effectively revealed, but defect 4 was not fully clear; the shape and deepness of defects could not be clearly judged, as with all surface NDT techniques. Furthermore, the shaker's location became self-evident and intrusive at 4800 Hz, a result that should be wisely excluded from any future automated defects' detection.

4.1. Defect tolerance based on full-field dynamic testing & Risk Index

The *damage location assessment* may play a relevant role in *defect tolerance strategies* combined with advanced *structural dynamics* and complex *excitation signature* sensing. As an example of the potentialities of a *coupled strategy*, the defects' location mapping of what just discussed, here as Zanarini (2021a), contains the *critical areas* to be the input of a *Risk Index map*, as obtained by ESPI *full-field dynamic testing* in Zanarini (2021b), from the *receptances* and their *derivatives* in Zanarini (2018, 2019a, 2021c). Therefore the location of each defect can tell if it can be accepted or not, in manufacturing or exercise, once the *complete real structural dynamics* and *excitation signature* are known. In this *coupled strategy*, *real defects' positions*, *structural dynamics & risk tolerance assessment* are all based on ESPI *full-field dynamic testing*, to put the most advanced testing knowledge into safety targets.

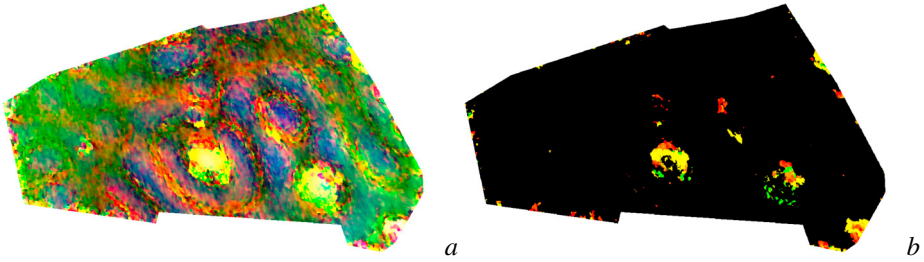

Fig. 8. Comparison of 3D data @ 4800 Hz - *sine shaker*: *raw* 3D data in *a*, *normalised thresholded* 3D data in *b*

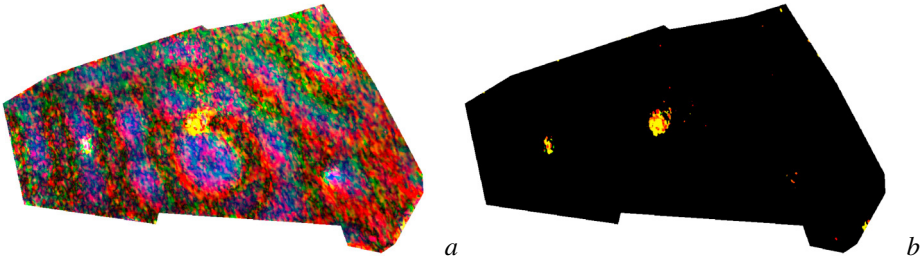

Fig. 9. Comparison of 3D data @ 5600 Hz - *sine shaker*: *raw* 3D data in *a*, *normalised thresholded* 3D data in *b*

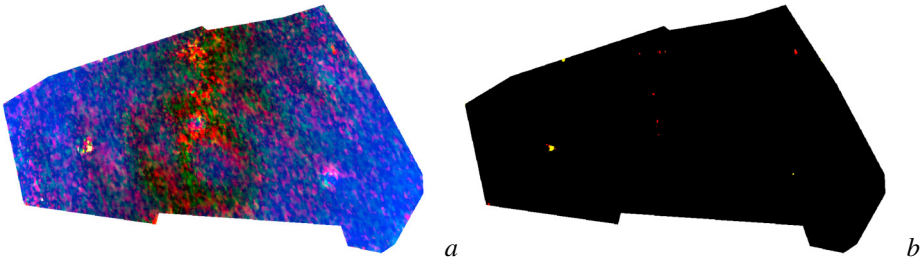

Fig. 10. Comparison of 3D data @ 5600 Hz - *sine shaker* + *static preload*: *raw* 3D data in *a*, *normalised thresholded* 3D data in *b*

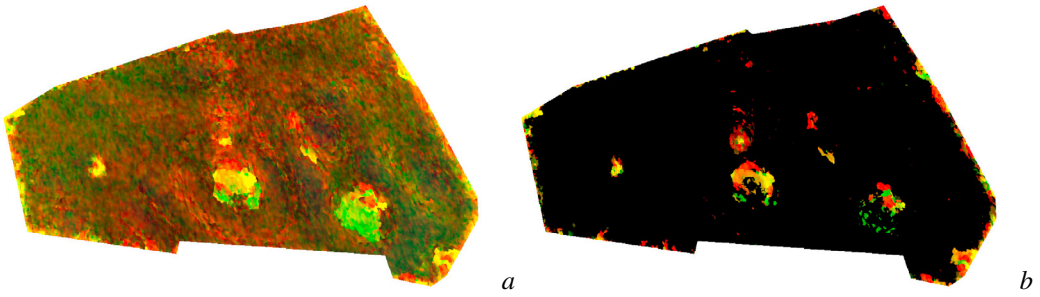

Fig. 11. Sum of *all* 3D data contributions: *raw* 3D data in *a*, *normalised thresholded* 3D data in *b*

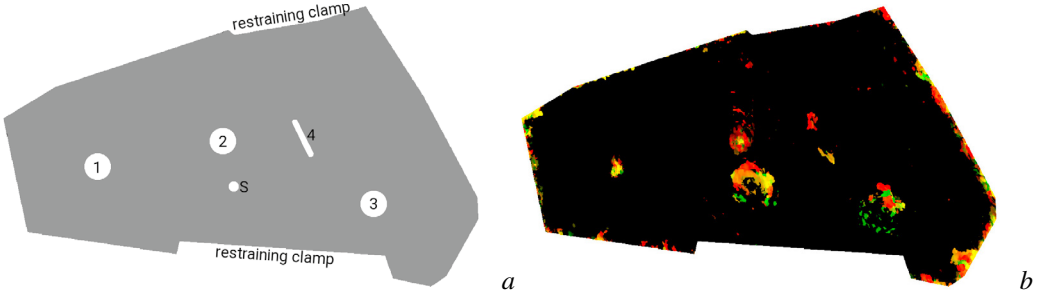

Fig. 12. Comparison of the defects' geometry with the sum of *all* 3D data normalised contributions: defects' location in *a*, sum of *normalised thresholded* 3D data in *b*

5. Conclusions

The extended studies of the *contactless full-field optical technologies* for NDT & structural dynamics have paved the path to the implementation of the simple *normalised thresholding* routine, here introduced, to enhance 3D data in the defected areas for a clearer automated detection. Great attention was put on the exploitation of the *in-plane* motions and on the *different* excitation sources, in terms of type and of frequency content, as needed by the different defects to self-reveal in the local behaviours as specific anomalies.

A satisfactory detection of the anomalies in the defected specimen was achieved with the proposed approach. This was another *proof-of-concept* about the chances provided by the *richness* & *continuity* of 3D optical full-field data in damage location assessment, promising for further enhancements in more sophisticated numerical routines. In particular, these were relevant outcomes for *coupled strategies* of *risk assessment* on components in production & exercise by means of optical full-field dynamic testing & NDT, to be further developed.

Acknowledgements

The European Commission Research Executive Agency is acknowledged for funding the HPMI-CT-1999-00029 *Speckle Interferometry for Industrial Needs* Post-doctoral Marie Curie Industry Host Fellowship project at Dantec Ettemeyer GmbH, Ulm, Germany, during the years 2004-2005; the latter for hiring the author in the project and for giving the author full access to their measuring equipment & lab facilities.

References

J. V. Araújo dos Santos, H. M. R. Lopes, M. Vaz, C. M. Mota Soares, C. A. Mota Soares, and M. J. M. de Freitas. Damage localization in laminated composite plates using mode shapes measured by pulsed TV holography. *Composite Structures*, 76(3):272–281, 2006. ISSN 0263-8223. https://doi.org/https://doi.org/10.1016/j.compstruct.2006.06.034. URL https://www.sciencedirect.com/science/article/pii/S0263822306002777. US Air Force Workshop Health Assessment of Composite Structures.

H. Lopes, J. V. Araújo dos Santos, and P. Moreno-García. Evaluation of noise in measurements with speckle shearography. *Mechanical Systems and Signal Processing*, 118:259 – 276, 2019. ISSN 0888-3270. https://doi.org/10.1016/j.ymssp.2018.08.042.

A. A. M. Maas. *Phase Shifting Speckle Interferometry*. PhD thesis, Delft University Press, 1991.

H. Van der Auweraer, H. Steinbichler, C. Haberstok, R. Freymann, D. Storer, and V. Linet. Industrial applications of pulsed-laser espi vibration analysis. In *Proc. of the XIX IMAC, Kissimmee, FL, USA*, pages 490–496. SEM, 2001. URL https://www.researchgate.net/publication/238246330_Industrial_Applications_of_Pulsed-Laser_ESPI_Vibration_Analysis.

A. Zanarini. Dynamic behaviour carachterization of a brake disc by means of electronic speckle pattern interferometry measurements. In *Proceedings of the IDETC/CIE ASME International Design Engineering Technical Conferences & Computers and Information in Engineering Conference, Long Beach, California, USA, September 24-28*, pages 273–280. ASME, 2005a. https://doi.org/10.1115/DETC2005-84630. Paper DETC2005-84630.

A. Zanarini. Damage location assessment in a composite panel by means of electronic speckle pattern interferometry measurements. In *Proceedings of the IDETC/CIE ASME International Design Engineering Technical Conferences & Computers and Information in Engineering Conference, Long Beach, California, USA, September 24-28*, pages 1–8. ASME, 2005b. https://doi.org/10.1115/DETC2005-84631. Paper DETC2005-84631.

A. Zanarini. Full field ESPI measurements on a plate: challenging experimental modal analysis. In *Proceedings of the XXV IMAC, Orlando (FL) USA, Feb 19-22*, pages 1–11. SEM, 2007. URL https://www.researchgate.net/publication/266896551_Full_field_ESPI_measurements_on_a_plate_Challenging_Experimental_Modal_Analysis. Paper s34p04.

A. Zanarini. Fatigue life assessment by means of full field ESPI vibration measurements. In P. Sas, editor, *Proceedings of the ISMA2008 Conference, September 15-17, Leuven (Belgium)*, pages 817–832. KUL, 2008a. https://doi.org/10.13140/RG.2.1.3452.9365. Condition monitoring, Paper 326.

A. Zanarini. Full field ESPI vibration measurements to predict fatigue behaviour. In *Proceedings of the IMECE2008 ASME International Mechanical Engineering Congress and Exposition, October 31- November 6, Boston (MA) USA*, pages 165–174. ASME, October 31- November 6 2008b. https://doi.org/10.1115/IMECE2008-68727. Paper IMECE2008-68727.

A. Zanarini. On the estimation of frequency response functions, dynamic rotational degrees of freedom and strain maps from different full field optical techniques. In *Proceedings of the ISMA2014 including USD2014 - International Conference on Noise and Vibration Engineering, Leuven, Belgium, September 15-17*, pages 1177–1192. KU Leuven, September 15-17 2014a. URL http://past.isma-isaac.be/downloads/isma2014/papers/isma2014_0676.pdf. Dynamic testing: methods and instrumentation, paper ID676.

A. Zanarini. On the role of spatial resolution in advanced vibration measurements for operational modal analysis and model updating. In *Proceedings of the ISMA2014 including USD2014 - International Conference on Noise and Vibration Engineering, Leuven, Belgium, September 15-17*, pages 3397–3410. KU Leuven, September 15-17 2014b. URL http://past.isma-isaac.be/downloads/isma2014/papers/isma2014_0678.pdf. Operational modal analysis, paper ID678.

A. Zanarini. Comparative studies on full field FRFs estimation from competing optical instruments. In *Proceedings of the ICoEV2015 International Conference on Engineering Vibration, Ljubljana, Slovenia, September 7-10*, pages 1559–1568. Univ. Ljubljana & IFToMM, September 7-10 2015a. URL https://www.researchgate.net/publication/280013709_Comparative_studies_on_Full_Field_FRFs_estimation_from_competing_optical_instruments. ID191.

A. Zanarini. Accurate FRFs estimation of derivative quantities from different full field measuring technologies. In *Proceedings of the ICoEV2015 International Conference on Engineering Vibration, Ljubljana, Slovenia, September 7-10*, pages 1569–1578. Univ. Ljubljana & IFToMM, September 7-10 2015b. URL https://www.researchgate.net/publication/280013778_Accurate_FRF_estimation_of_derivative_quantities_from_different_full_field_measuring_technologies. ID192.

A. Zanarini. Full field experimental modelling in spectral approaches to fatigue predictions. In *Proceedings of the ICoEV2015 International Conference on Engineering Vibration, Ljubljana, Slovenia, September 7-10*, pages 1579–1588. Univ. Ljubljana & IFToMM, September 7-10 2015c. URL https://www.researchgate.net/publication/280013788_Full_field_experimental_modelling_in_spectral_approaches_to_fatigue_predictions. ID193.

A. Zanarini. Model updating from full field optical experimental datasets. In *Proceedings of the ICoEV2015 International Conference on Engineering Vibration, Ljubljana, Slovenia, September 7-10*, pages 773–782. Univ. Ljubljana & IFToMM, September 7-10 2015d. URL https://www.researchgate.net/publication/280013876_Model_updating_from_full_field_optical_experimental_datasets. ID196.

A. Zanarini. Broad frequency band full field measurements for advanced applications: Point-wise comparisons between optical technologies. *Mechanical Systems and Signal Processing*, 98:968 – 999, 2018. ISSN 0888-3270. https://doi.org/10.1016/j.ymssp.2017.05.035.

A. Zanarini. Competing optical instruments for the estimation of Full Field FRFs. *Measurement*, 140:100 – 119, 2019a. ISSN 0263-2241. https://doi.org/10.1016/j.measurement.2018.12.017.

A. Zanarini. Full field optical measurements in experimental modal analysis and model updating. *Journal of Sound and Vibration*, 442:817 – 842, 2019b. ISSN 0022-460X. https://doi.org/10.1016/j.jsv.2018.09.048.

A. Zanarini. On the making of precise comparisons with optical full field technologies in NVH. In *Proceedings of the ISMA2020 including USD2020 - International Conference on Noise and Vibration Engineering, Leuven, Belgium, September 7-9*, pages 2293–2308. KU Leuven, September 7-9 2020. URL https://www.researchgate.net/publication/344353185_On_the_making_of_precise_comparisons_with_optical_full_field_technologies_in_NVH. Optical methods and computer vision for vibration engineering, paper ID 695.

A. Zanarini. On the exploitation of multiple 3D full-field pulsed espi measurements in damage location assessment. *Procedia Structural Integrity*, pages 1–8, 2021a. ISSN 2452-3216. paper ID 104, ICSI 2021 The 4th International Conference on Structural Integrity.

A. Zanarini. On the defect tolerance by fatigue spectral methods based on full-field dynamic testing. *Procedia Structural Integrity*, pages 1–8, 2021b. ISSN 2452-3216. paper ID 105, ICSI 2021 The 4th International Conference on Structural Integrity.

A. Zanarini. Chasing the high-resolution mapping of rotational and strain FRFs as receptance processing from different full-field optical measuring technologies. *Mechanical Systems and Signal Processing*, page 108428, 2021c. ISSN 0888-3270. https://doi.org/10.1016/j.ymssp.2021.108428. Accepted on September 3rd 2021, online from September 25th, YMSSP108428.